

Effect of the phospholipid head group in antibiotic-phospholipid association at water–air interface

F. Gambinossi^{a,*}, B. Mecheri^a, M. Nocentini^b, M. Puggelli^a, G. Caminati^a

^a*Dipartimento di Chimica, Polo Scientifico – Università di Firenze – Via della Lastruccia, 3, 50019 Sesto Fiorentino, Firenze, Italy*

^b*Istituto Zooprofilattico Sperimentale delle Regioni Lazio e Toscana-Dipartimento di Firenze-Via di Castelpulci 41, 50010 San Martino alla Palma, Firenze, Italy*

Received 11 November 2003; received in revised form 22 January 2004; accepted 23 January 2004
Available online 5 May 2004

Abstract

We studied the interactions of tetracycline antibiotics, TCs, with phospholipid monolayers with the two-fold aim of elucidating the mechanism of action of TCs and to provide a first step for the realization of bio-mimetic sensor for such drugs by means of the Langmuir–Blodgett technique. Preliminary surface tension studies demonstrated that surface activity of tetracycline is moderate and dependent on the pH of the subphase. We selected three phospholipids having hydrophobic chains of the same length but differing in the polar head structures, i.e. dipalmitoylphosphatidylcholine, dipalmitoylphosphatidylethanolamine, and dipalmitoylphosphatidic acid. Surface pressure- and surface potential- area isotherms were employed to investigate the behavior of the phospholipid monolayers at the water–air interface when tetracycline was added to the aqueous subphase. Analysis of the results indicated that the electrostatic interaction is the driving force for migration of tetracycline towards the interface where localized adsorption to the head groups occurs. Nevertheless, such interactions appear to be insufficient to promote penetration of tetracycline through the hydrophobic layer.

© 2004 Elsevier B.V. All rights reserved.

Keywords: Tetracyclines; Phospholipids; Monolayers; Surface tension; Surface pressure; Surface potential

1. Introduction

Tetracyclines are a subclass of the polyketide antibiotics that contain an octahydrotetracene-2-carboxamide skeleton substituted with numerous hydroxyl and other functionalities. These molecules

are broad-spectrum antibiotics acting on gram-positive and gram-negative strains, mycoplasmas as well as some protozoa. Tetracyclines, extensively used as veterinary antibiotics, survive the manufacturing cycle and contaminate animal-derived foods. The presence of their residues in edible products of animal origin can pose serious problems to human health inducing allergic syndrome and, even more importantly, strain resistance in the population. Since current international legislations impose a limit concentration for tetracyclines in food, much effort is

* Corresponding author. Tel.: +39-055-4573024; fax: +39-055-4573385.

E-mail addresses: gambinossi@csgi.unifi.it (F. Gambinossi), caminati@unifi.it (G. Caminati).

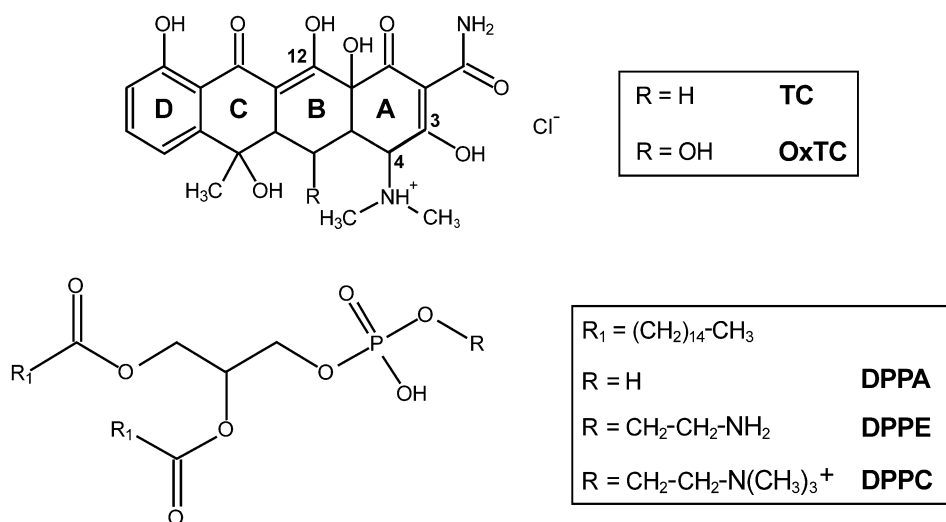


Fig. 1. Chemical structures of the tetracyclines and of the selected phospholipids.

devoted to clarify their mechanism of action and to develop sensors for ultra low concentration of these compounds.

The mechanism of action of these drugs has been generally related to their ability to penetrate through biological membranes [1] but a detailed comprehension of such process is still in its infancy. Whereas many works deal with the interactions of drug molecules such as antibiotics [2,3], or anaesthetics [4,5] with phospholipid monolayers, reports on tetracyclines are scarce. A previous study demonstrated that tetracycline interacts with phospholipids such as phosphatidylethanolamine [6], but little is known on the details of such processes. Therefore, it appears particularly important to understand the mechanism of interaction between tetracyclines and Langmuir monolayers of phospholipids, which are well known to act as simple although representative models of biomembranes [7,8].

In this paper, we focused on the study of spreading monolayer of three typical phospholipid constituents of natural membranes in the presence of tetracycline in the subphase. We have selected dipalmitoylphosphatidylcholine, DPPC, dipalmitoylphosphatidylethanolamine, DPPE and dipalmitoylphosphatidic acid, DPPA, as native monolayers. The three phospholipids have hydrophobic chains of the same length but polar groups differing either in dimensions and protonation

equilibria. Inspection of surface pressure and surface potential isotherms provided a powerful tool to monitor drug–lipid interactions determining changes in the distribution and orientation of the phospholipids at water–air interface induced by the drug. These studies allowed to specify the mode of interaction and to estimate the percentage of antibiotic incorporated in the monolayer.

This paper is part of a systematic work on the study of the interactions of tetracycline antibiotics with phospholipid monolayers at water–air interface that would eventually provide not only further insight in their mechanism of action but also a key indication for the realization of mimetic sensor for such drugs.

2. Experimental

2.1. Materials

Tetracycline hydrochloride (TC) and Oxytetracycline (OxTC) were supplied by Sigma, the purity is >99%, and the molecular weight is 481 for TC and 497 for OxTC. Dipalmitoylphosphatidic acid (DPPA), dipalmitoylphosphatidylcholine (DPPC) and dipalmitoylphosphatidylethanolamine (DPPE) were supplied by Sigma; the purity is >99% for all the three phospholipids. The chemical structures

of TC, OxTC, DPPA, DPPC and DPPE are reported in Fig. 1. Chloroform was used as spreading solvent for DPPC and DPPA, whereas chloroform/methanol mixtures (10/1 v/v) were used for DPPE spreading solutions, both solvents were supplied by Aldrich. Phospholipid concentration of 1×10^{-3} M was typically used for spreading solutions, unless otherwise stated in the text; solution volumes in the range 100–200 μ l were spread on the surface using a Hamilton syringe. Water was obtained from a Milli-RO coupled with a Milli-Q set-up (Millipore): resistivity 18.2 M Ω cm, pH 5.6 at 20 $^{\circ}$ C.

2.2. Methods

Surface tension, γ , measurements were obtained with the Du Nouy method using a Mettler balance with a platinum ring ($\varnothing=2$ cm) immersed in a trough containing the solution to be examined at controlled temperature. Surface tension was measured as a function of TC in the subphase at 20 and 25 $^{\circ}$ C; TC concentration was varied by standard additions of aliquots of a stock solution ($[TC]=10^{-2}$ M) and 30 min were allowed for equilibration before each γ measurement. Surface pressure–surface area, π – A , isotherms were obtained with a Lauda Filmwaage FW2 (Lauda, Germany) by discontinuous compression. Spreading isotherms were obtained at 20 $^{\circ}$ C using a Haake thermostat with water circulation bath. The compression rate was 8 $\text{\AA}^2 \text{ molecule}^{-1} \text{ min}^{-1}$; three π values were recorded for each surface area with a time interval of 30 s between the measurements, only the last π measurement is reported in the isotherms. 30 min were allowed for solvent evaporation and tetracycline equilibration at the interface prior compression. All the spreading isotherms of DPPA, DPPE, and DPPC shown in this paper are the average of at least three curves. Surface potential–surface area, ΔV – A , measurements were obtained with the method of the ionizing electrode by using ^{241}Am electrodes, with an apparatus assembled in the Department of Chemistry (Florence) and previously described [9,10]. The accuracy of γ was $\pm 0.1 \text{ mN m}^{-1}$, of π was $\pm 0.1 \text{ mN m}^{-1}$, of A was $\pm 0.5 \text{ \AA}^2 \text{ molecule}^{-1}$ and of ΔV was $\pm 10 \text{ mV}$. Semi-empirical calculations (PM3, AM1) [11,12]

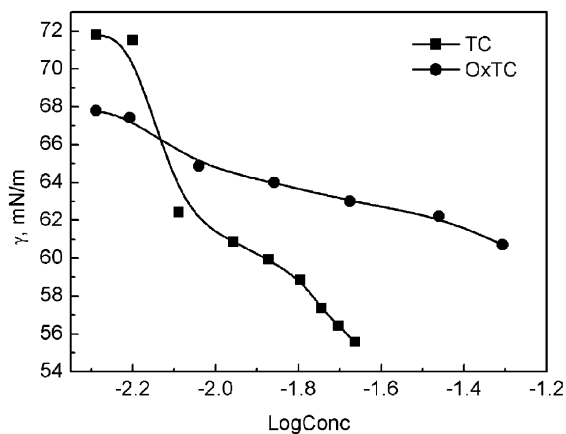


Fig. 2. Adsorption isotherms at 25 $^{\circ}$ for TC and OxTC.

were run using the software HyperChem 5.1 (HyperCube, USA).

3. Results and discussion

3.1. Tetracycline adsorption isotherms at water/air interface

At 20 $^{\circ}$ C adsorption isotherms of TC could be determined only for concentration lower than 10^{-2} M whereas at 25 $^{\circ}$ C adsorption isotherms for TC were recorded only in the concentration range 6×10^{-3} – 2×10^{-2} M. γ values at higher TC concentrations are not reliable because of incipient precipitation and were discarded. A similar γ behavior was found at both temperatures: a decrease of surface tension was observed for tetracycline concentrations higher than 5×10^{-3} M. Typical adsorption isotherms of TC and of OxTC at water–air interface, at 25 $^{\circ}$ C, are reported in Fig. 2. Comparison between the two curves shows that the overall drop in surface tension is higher for TC than for OxTC, indicating that adsorption at the interface is favoured for TC. This behavior can be explained with the higher solubility of OxTC in water, which strongly competes with the adsorption process. Adsorption isotherm for OxTC shows a continuous decrease of γ as a function of concentration, without any clear-cut discontinuity, as in the case of poorly surface-active substances. An initial drop followed by a linear region characterizes γ – $\log[TC]$ curve, these features can be rationalized in terms of differently

protonated TC species in solution. The behavior of the tetracycline family in water solution is complex and involves protonation and pH-dependent conformational equilibria; most of the existing studies are focused on TC, whereas little is known on OxTC. In particular, TC exhibits three main macroscopic acidity constants, the assignment of which has been widely accepted [13,14]. The first deprotonation is ascribed to the OH3 group in the A ring, whereas the second deprotonation involves the OH12 group on the B ring and only the third deprotonation is associated with the dimethylamino group in the A ring (see Fig. 1). The corresponding pK_s determined either by potentiometric or spectroscopic methods are $pK_1=3-4$, $pK_2=7-8$, $pK_3=8.8-9.8$ [13–16].

The protonation equilibria of TC molecule induce also a change of molecular conformation: in acidic to neutral solution (below $pH=8$) TC adopts a twisted conformation in order to relieve the steric crowding between the protonated nitrogen on the dimethylamino group, NH_4 , and the OH12. In this conformation, which is usually referred as folded conformation [13,14,17], the dimethylamino group lies above the BCD ring system. Increasing pH the conformational equilibrium is shifted towards the extended conformation, where the dimethylamino group lies below the plane spanned by the BCD ring system.

We observed a decrease of the experimental pH with the increase in [TC], the distribution of the different protonated TC species at each pH was computed using Eq. (1) considering the activity coefficient as unity:

$$\alpha_{ni} = \frac{\beta_i \cdot [H^+]^i}{\sum_{j=0}^n \beta_j \cdot [H^+]^j}; \quad 0 \leq i \leq n \quad (1)$$

where n is the total number of protons available for each species i , β values are the global basicity constants, correlated to the acid constant, K by the expression:

$$\beta_0 = 1; \quad \beta_i = \prod_{j=1}^i \left(\frac{1}{K_{n+1-j}} \right) \quad (2)$$

The pK values for TC, used for our calculations, are $pK_1=3.3$, $pK_2=7.68$ and $pK_3=9.69$ [18].

Table 1

Experimental pH values, distribution of tetracycline and DPPA species in the TC concentration range $0-5 \times 10^{-3}$ M

[TC], M	pH _{exp}	$\alpha_{H_4TC^+}$	α_{H_3TC}	α_{HDPPA^-}
0	5.66			0.69
1×10^{-6}	5.23	0.01	0.98	0.85
5×10^{-6}	4.99	0.02	0.98	0.91
5×10^{-5}	4.27	0.10	0.90	0.98
1×10^{-4}	4.05	0.15	0.85	0.98
5×10^{-4}	3.44	0.42	0.58	0.96
2×10^{-3}	3.04	0.65	0.35	0.92
5×10^{-3}	2.78	0.77	0.23	0.86

The results reported in Table 1 show that only the totally protonated form, H_4TC^+ , and the neutral form, H_3TC , are present in significant population in the range of [TC] investigated, whereas the fraction of the negatively charged molecule, H_2TC^- , is negligible. With increasing [TC] the equilibrium among the different species moves towards the protonated form in the folded conformation. These data were confirmed by circular dichroism studies [19] indicating that the totally protonated species is present as 99% in solution at $pH=1$ whereas the neutral form is only 1%. These considerations may explain surface tension behavior for tetracycline: after the initial γ drop, we observe a discontinuity in the γ -log[TC] curve corresponding to the cross-over to a regime, where basically only H_4TC^+ is present. At concentrations higher than 1.5×10^{-2} M precipitation of TC hinders further interpretation of the results. The change in the slope of γ -log[TC] curve may indicate that surface activity of tetracycline decreases with increasing pH. Similar trends in γ were observed also for colistine, dibucaine [3,20] and antimalarial drugs [21], all these molecules are differently protonated as a function of pH.

The surface excess and the molecular area for compact monolayers of tetracycline at the interface were determined from γ measurements applying the Gibbs adsorption isotherm in the linear portions of the curve:

$$\Gamma_{TC} = - \frac{C_{TC}}{nRT} \cdot \left(\frac{\partial \gamma}{\partial C_{TC}} \right)_T \quad (3)$$

where $n=1$ for non-ionic compounds and $n=2$ [22], for singly charged substances. The surface area per TC molecule is inversely proportional to Γ_{TC} . Application of Eq. (3) to the first region of the γ -log[TC] curve

was attempted considering that only the H_3TC form contributes to the adsorption layer ($n=1$), in this case we found a surface area of $12 \text{ \AA}^2 \text{ molecule}^{-1}$. However, using $n=2$, we obtain a molecular area of $24 \text{ \AA}^2 \text{ molecule}^{-1}$. Both these unrealistically small values suffer of a heavy approximation since both H_3TC and H_4TC^+ species are present in this concentration range (see Table 1). In the second linear portion of the curve, i.e. $[\text{TC}] > 8.5 \times 10^{-3} \text{ M}$ corresponding to $\text{pH} < 2.1$, the charged species is largely predominant in solution and application of Eq. (3) gave a molecular area of $158 \text{ \AA}^2 \text{ molecule}^{-1}$ for tetracycline.

This area value was compared with the molecular dimensions obtained from geometry optimization of TC in vacuo using both PM3 and AM1 calculations; the molecular structure of H_4TC^+ , in the folded conformation after energy minimization is reported in Fig. 3. In the case depicted in Fig. 3, we computed a cross-sectional area of 97 \AA^2 from the molecular dimensions with D–C–B rings of the molecule almost parallel to the interface. Other possible conformations, with the long axis of the molecule perpendicular to the interface, would provide much smaller cross-sectional areas, i.e. 80 and 47 \AA^2 . These conformations were disregarded since we considered a vertical disposition, with most of the oxygen atoms sticking out of the surface, as highly unlikely. In any case, area values of 12 \AA^2 or 24 \AA^2 per TC molecule are indeed unrealistically small, on the contrary the value of 158 \AA^2 obtained per H_4TC^+ molecule in the adsorption layer nicely supports the picture of the horizontal orientation of the molecule; the difference between the geometrical and the experimental value may possibly be attributed to electrostatic repulsion between charged molecules. The invariance of surface activity for low TC concentrations was confirmed also by surface pressure measurements on subphase containing $[\text{TC}] < 5 \times 10^{-3}$: π was recorded in the absence of any amphiphilic monolayer but no significant increase of π was recorded even at maximum compression.

3.2. π - A isotherms at water–air interface

The spreading isotherms of the selected phospholipids on water subphase and on subphases containing tetracycline in the concentration range 10^{-6} – $5 \times 10^{-3} \text{ M}$ are reported in Figs. 4–6 for DPPC, DPPE and DPPA, respectively. π - A isotherms for the three

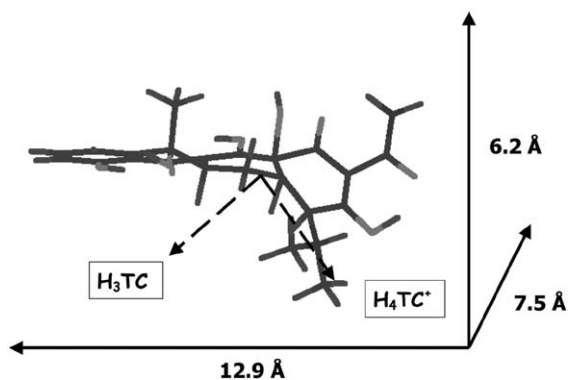


Fig. 3. Molecular structure and estimated dimensions for H_4TC^+ in folded conformation.

phospholipids on water (not shown here) are in good agreement with those previously reported [23–25]. As reported in Section 3.1, tetracycline is not surface active in the concentration range studied and any change in π can be safely ascribed to interactions between TC and the lipid molecules.

Observation of the experimental results allows to identify a discontinuity in the behavior of the isotherms at a threshold concentration of tetracycline, $[\text{TC}]^*$, whose values are reported in Table 2 for the three phospholipids. In the same table we also report the main parameters extracted from the isotherms, i.e. the limiting molecular area A_0 , the collapse surface pressure π_C and the maximum surface compressional modulus C_S^{-1} for the two regimes. A_0 is determined extrapolating the linear portion in the condensed region of the isotherm to zero surface pressure, π_C is taken as the surface pressure corresponding to the point where the slope of the isotherm abruptly changes, and C_S^{-1} is defined as [26]:

$$C_S^{-1} = -A \cdot \left(\frac{\partial \pi}{\partial A} \right)_T \quad (4)$$

It is evident from the figures and from the parameters reported in Table 2 that tetracycline affects to different extent the isotherms of the three phospholipids. At any rate, changes in π - A isotherms cannot be ascribed to a mere pH effect on the phospholipid behavior since it is well known that for DPPC and DPPE only slight condensation of the monolayer would be expected with decreasing pH, i.e. with increasing TC concentration. The same holds for DPPA

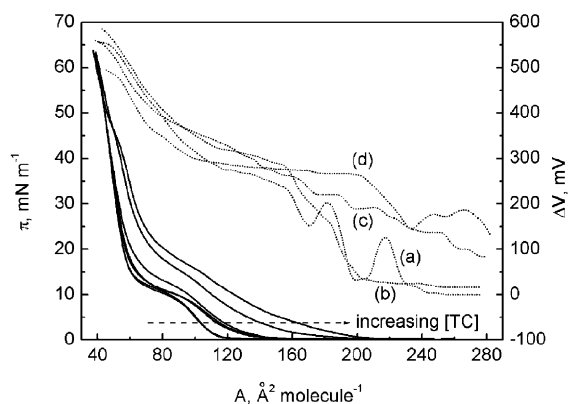


Fig. 4. Surface pressure (solid lines) and surface potential (dotted lines) vs. molecular areas of DPPC at 20 °C on subphases containing tetracycline in the concentration range $0-5 \times 10^{-3}$ M. (a) 1×10^{-6} M; (b) 5×10^{-6} M; (c) 5×10^{-4} M; (d) 5×10^{-3} M.

monolayers, for which an abrupt expansion of $\pi-A$ curves is reported to occur only at $\text{pH} > \text{p}K_2 = 6$ [27].

DPPC isotherms (see Fig. 4) move toward higher molecular areas increasing tetracycline concentration in the subphase, particularly above $[\text{TC}]^*$, this shift is accompanied by an increase in the surface pressure corresponding to the LC–LE phase transition. The ‘expansion effect’ due to tetracycline is more important in the liquid expanded phase, as confirmed by the maximum surface compressional modulus at $\pi = 5 \text{ mN m}^{-1}$. At higher surface pressure the effect is reduced and a kink can be observed at $\pi_k = 45-50 \text{ mN m}^{-1}$; after this surface pressure the curves almost superimpose for all tetracycline concentrations. Moreover, all the spreading isotherms for DPPC show similar collapse surface pressure; the limiting areas remain constant up to $[\text{TC}]^*$ and only beyond this concentration A_0 increases. This behavior suggests that tetracycline is ‘forced out’ of the monolayer at close packing of DPPC monolayer. Accumulation at boundaries between fluid and condensed domains of DPPC monolayer is phenomenon frequently observed [28]; in this specific case tetracycline appears to be effectively excluded from highly condensed DPPC phases.

Surface pressure–area behavior for DPPE spread on an aqueous subphase containing tetracycline is similar to what observed on water subphase for $[\text{TC}] \leq [\text{TC}]^*$ as reported in Fig. 5. Above $[\text{TC}]^*$ a phase transition appears in the $\pi-A$ curves around $\pi = 5 \text{ mN m}^{-1}$ and the isotherms shift towards larger areas. The expansion of

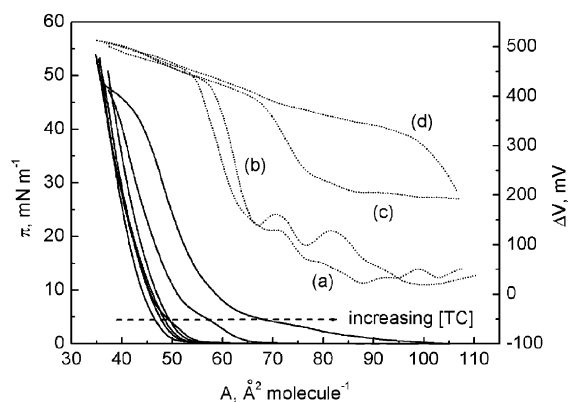


Fig. 5. Surface pressure (solid lines) and surface potential (dotted lines) vs. molecular areas of DPPE at 20 °C on subphases containing tetracycline in the concentration range $0-5 \times 10^{-3}$ M. (a) 1×10^{-6} M; (b) 5×10^{-5} M; (c) 2×10^{-3} M; (d) 5×10^{-3} M.

DPPE monolayer with increasing TC concentration is confirmed also by the values of the surface compressional modulus (see Table 2). Moreover, the limiting area value increases and π_{coll} decreases, these features suggest that tetracycline remains incorporated into the monolayer or in the electrical surface double layer upon monolayer compression.

A completely different picture emerges from the observation of $\pi-A$ for DPPA monolayers on subphases containing tetracycline (see Fig. 6). In this case, the spreading isotherms show a substantial displacement to higher values of surface area already at low

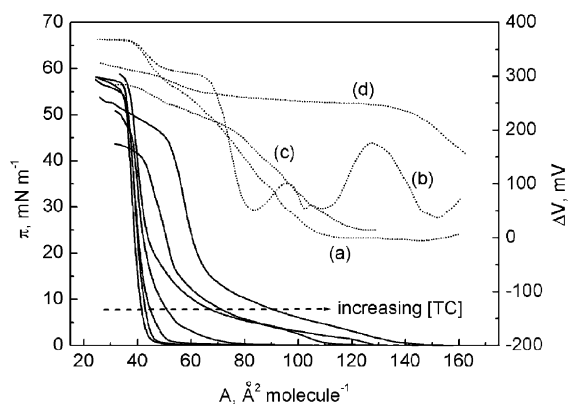


Fig. 6. Surface pressure (solid lines) and surface potential (dotted lines) vs. molecular areas of DPPA at 20 °C on subphases containing tetracycline in the concentration range $0-5 \times 10^{-3}$ M. (a) 1×10^{-6} M; (b) 5×10^{-5} M; (c) 1×10^{-4} M; (d) 5×10^{-3} M.

Table 2
Monolayer parameters extracted from π – A isotherms

	[TC]*, M	A_0 , Å ² molecule ^{−1}			π_C , mN m ^{−1}			C_S^{-1} , mN m ^{−1}					
		[TC]=0	[TC]≤[TC]*	[TC]>[TC]*	[TC]=0	[TC]≤[TC]*	[TC]>[TC]*	$\pi=5$ mN m ^{−1}			$\pi=35$ mN m ^{−1}		
								[TC]=0	[TC]≤[TC]*	[TC]>[TC]*	[TC]=0	[TC]≤[TC]*	[TC]>[TC]*
DPPC	5×10 ^{−4}	64	64	73	63	62(63) ^a	64	43	33 (29) ^a	18	152	132 (110) ^a	84
DPPE	5×10 ^{−4}	41	45	58	52	52(50) ^a	42	95	100 (51) ^a	20	228	224 (241) ^a	129
DPPA	1×10 ^{−4}	40	43 (45) ^a	68	54	57(46) ^a	46	159	56 (29) ^a	14	358	270 (238) ^a	150

^a[TC]<[TC]* ([TC]=[TC]*).

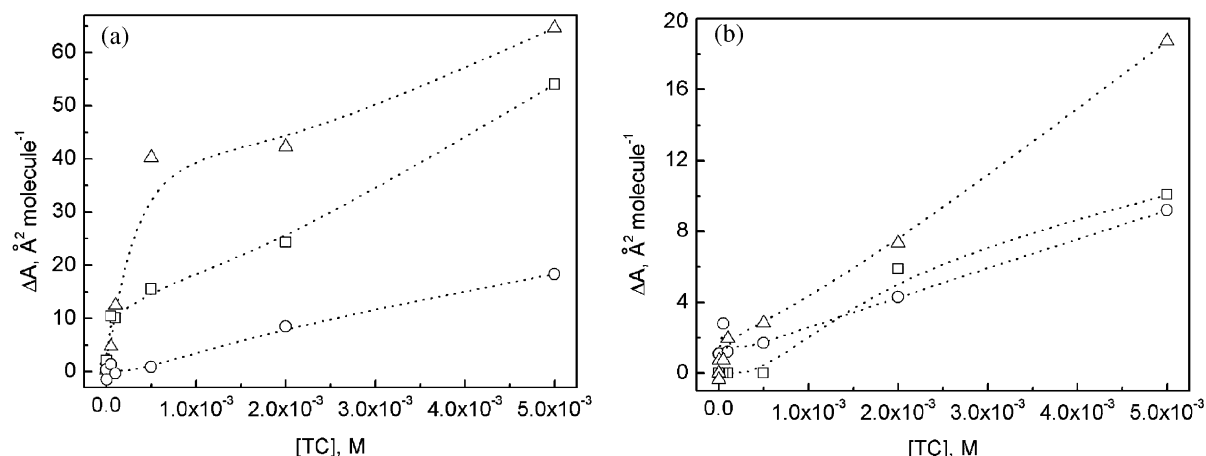


Fig. 7. Difference in surface areas at constant π between phospholipid monolayer on subphase containing tetracycline and on water subphase: DPPC (squares), DPPE (circles), DPPA (upward triangles). (a) $\pi=5$ mN m $^{-1}$; (b) $\pi=35$ mN m $^{-1}$.

[TC] with a significant increase in the limiting area at the highest tetracycline concentration. Collapse surface pressure remains constant for $[TC] \leq [TC]^*$ and then decreases as a function of TC content. The shape of the isotherms in the expanded phase changes for TC concentrations as low as 1×10^{-4} M suggesting the appearance of a liquid expanded phase at low DPPA density. Moreover, upon further compression the monolayer remains more expanded compared to water subphase as evidenced by the maximum C_S^{-1} reported in Table 2.

The above findings indicate that tetracycline strongly affects the behavior of DPPA monolayer, whereas DPPC and DPPE interact more weakly with the antibiotic. The threshold tetracycline concentration value, $[TC]^*$, at which we observe an appreciable variation in the π – A isotherms is different for the three phospholipids (see Table 2) and the extent of such variation depends exclusively on the anchoring polar group which appear to be directly involved in the interactions with tetracycline.

This effect is more clearly described in Fig. 7 where we present ΔA as a function of tetracycline concentration. $\Delta A = A_{\text{Lip-TC}} - A_{\text{Lip}}$ is calculated at constant surface pressure as the difference between the molecular areas of the phospholipid on subphases containing tetracycline and on water subphase. We separately examined the expanded phase domain, i.e. $\pi=5$ mN m $^{-1}$ (Fig. 7a), and the condensed one, i.e. $\pi=35$ mN m $^{-1}$ (Fig. 7b). In this latter region the

variation is considerably smaller than in the former one, but in both phase domains, we again observe a discontinuity in the increase of surface area at $[TC]^*$.

Preferential interactions with the phospholipids monolayer in the expanded phase were also found for proteins incorporation by other authors [29,30].

The critical concentration can be related to the distribution of TC species reported in Table 1: below $[TC]^*$ the neutral form H_3TC is predominant in solution. The small area variation seems to indicate that this species does not interact significantly with DPPE, neither in the expanded nor in the condensed phase; interactions are slightly higher for DPPC before the LE–LC phase transition.

On the contrary, larger area changes were observed for DPPA even if a ΔA value of 12 \AA^2 for DPPA molecule is still too small to be interpreted as a significant H_3TC insertion in the monolayer, the increase of ΔA could simply involve a perturbation of the hydrogen-bond network induced by adsorption of tetracycline underneath the polar head groups of the phospholipid.

Above $[TC]^*$, H_3TC is replaced by H_4TC^+ and ΔA increases considerably in the case of DPPA, final values of 60 \AA^2 molecule $^{-1}$ and 20 \AA^2 molecule $^{-1}$ are observed at $\pi=5$ mN m $^{-1}$ and $\pi=35$ mN m $^{-1}$, respectively. Although ΔA increases steadily also for DPPC and DPPE above $[TC]^*$, the maximum ΔA values observed are always much smaller than in the case of DPPA.

Table 3

Phospholipid/TC molar ratio, n , calculated from π - A isotherms, for DPPE, DPPC and DPPA both in the expanded phase ($\pi=5$ mN m⁻¹) and in the condensed one ($\pi=35$ mN m⁻¹)

[TC], M	$\pi=5$ mN m ⁻¹			$\pi=35$ mN m ⁻¹		
	$n_{\text{DPPC}}/n_{\text{TC}}$	$n_{\text{DPPE}}/n_{\text{TC}}$	$n_{\text{DPPA}}/n_{\text{TC}}$	$n_{\text{DPPC}}/n_{\text{TC}}$	$n_{\text{DPPE}}/n_{\text{TC}}$	$n_{\text{DPPA}}/n_{\text{TC}}$
1×10^{-6}	>100	>100	>100	>100	91	>100
5×10^{-6}	46	>100	48	>100	91	>100
5×10^{-5}	10	>100	21	>100	36	37
1×10^{-4}	10	>100	8	>100	83	51
5×10^{-4}	6	100	2.5	>100	59	35
2×10^{-3}	4	12	2.5	17	23	14
5×10^{-3}	2	6	1.5	10	11	5

An estimate of the concentration of antibiotic at the interface was attempted comparing the ΔA values with the geometrical requirements for tetracycline obtained from molecular modelling and assuming that the molecule adopts a flat conformation with the BCD rings parallel to the interface and the oxygen rich region interacting with hydrophilic layer, i.e. tetracycline cross-sectional area $\approx 100 \text{ \AA}^2$. The molar ratio between the amphiphilic molecules and tetracycline at the interface was calculated as:

$$\frac{n_{\text{lipid}}}{n_{\text{TC}}} = \frac{vA_{\text{TC}}}{\Delta A} \quad (5)$$

and the results are reported in Table 3 for the three phospholipids and at two surface pressures, i.e. 5 and 35 mN m⁻¹. Above [TC]*, a cross-sectional area of 158 \AA^2 was also considered in analogy with surface tension results and we found an average increase of 60% in $\frac{n_{\text{lipid}}}{n_{\text{TC}}}$.

For low TC concentrations, the phospholipids/tetracycline ratio is always large for all the phospholipids examined, especially for DPPE in the expanded phase. After the threshold concentration $\frac{n_{\text{lipid}}}{n_{\text{TC}}}$ decreases but we observe a significant presence of tetracycline at the interface only for DPPA in the expanded phase reaching an average of two DPPA molecules for each TC.

Above [TC]*, we have already seen that the charged species H_4TC^+ is the predominant one in solution and that the charged form is less surface active than the neutral one, therefore the decrease in $\frac{n_{\text{lipid}}}{n_{\text{TC}}}$ indicates that TC interactions with the phospholipids are strongly enhanced by electrostatic attraction of the positive charge towards the negative diffuse charge localized in the region of the phosphorus

atoms. Moreover, DPPA undergoes protonation–deprotonation equilibria, from the values reported in Table 1 it can be easily seen that the HDPPA^- species is always the predominant one and its maximum concentration occurs at pH=4. On the contrary, zwitterionic phospholipids remain unaltered in the pH range investigated but tetracycline effect is much smaller for the DPPC and DPPE. Although the charged H_4TC^+ species interacts more favourably with either the choline and ethanolamine moieties compared to H_3TC , the increase in ΔA is small especially for closed packed monolayers and vanishes in the case of DPPC above $\pi=50$ mN m⁻¹.

These results indicate that tetracycline interacts with the three phospholipid monolayers but differently in each case. This difference appears to be dictated by charge density and protonation equilibria at the interface. From the above data, it seems highly unlikely that tetracycline may penetrate the hydrophobic portion of the monolayer in condensed monolayer phases. Localized adsorption at the phospholipid head group appear like a possible mechanism as reported by other authors for several drugs bearing charged amino groups [31,32]. In the case of the anaesthetic chlorpromazine, the authors [33] demonstrated drug penetration in the lipid layer with relative changes in molecular areas $\Delta A/A$ in the range 5–15%. The results reported in Table 3 for DPPE and DPPC correspond at most to a relative change always much lower than 5%, only for DPPC fluid phase we obtain an association of 20% tetracycline. For DPPA we obtain 20–30% insertion in the expanded phase and 5–10% in the condensed phase, this confirms that the antibiotic remains at least loosely associated to the monolayer

also at high π in the case of DPPA and DPPE but not for DPPC.

3.3. ΔV – A measurements at water–air interface

3.3.1. General analysis for tetracycline-free subphases

Experimental ΔV values obtained for the three phospholipids on water (not shown here) compare well with the literature reports on the same compounds [34,35]. Surface potential, ΔV , provides a description of the electric dipole density at the water–air interface and it is generally described [9] as:

$$\Delta V = \Delta V_{\text{dip}} + \Psi_0 \quad (6)$$

where the term ΔV_{dip} is due to the permanent dipole moment of the amphiphilic molecule and Ψ_0 , i.e. the double layer potential, is present only in the case of ionized or ionisable monolayer.

For what concerns DPPC and DPPE, the term Ψ_0 in Eq. (6) is null in the entire TC concentration range considered since the variation of pH induces negligible changes in ionization of the polar group of phosphatidylcholine and of phosphatidylethanolamine [34,36]. For the two zwitterionic phospholipids we also considered that $\Delta V = \Delta V_{\text{dip}}$ is unaffected by the variation of pH in the subphase [34,36].

In the case of DPPA monolayers, the Ψ_0 term cannot be neglected, and it was computed using the Gouy–Chapman theory [22,26,37]:

$$\Psi_0 = \frac{2kT}{e} \cdot \sinh^{-1} \left(\frac{\sigma}{(8\epsilon\epsilon_0 kTc)^{1/2}} \right) \quad (7)$$

where k is Boltzmann's constant, T the absolute temperature, ϵ and ϵ_0 are the local and vacuum relative permittivity. σ , the surface charge density, is equal to $e\alpha/A$ with e the electronic charge, α the degree of the dissociation of the head group, A the area per molecule, c the ionic concentration of the subphase (M). α was calculated using Eq. (1) with literature values for the average interfacial pKs: $\text{p}K_1=2$ and $\text{p}K_2=6$ [38]. Ψ_0 values were obtained neglecting DPPA^{2−} species contribution and are reported in Table 4.

The contribution due to DPPA at the interface at [TC]=0 (pH=5.7) was obtained from the experimental ΔV isotherms and Ψ_0 was calculated as $\Delta V_{\text{dip}}^{\text{Lipid}} = (\Delta V - \Psi_0)$ from Eq. (6).

The term ΔV_{dip} in Eq. (6) is correlated to the vertical component of the dipole moment, μ_{\perp} , of the amphiphile forming the monolayer [9]:

$$\Delta V_{\text{dip}} = \frac{n\mu_{\perp}}{\epsilon\epsilon_0} = \frac{\vec{\mu} \langle \cos\vartheta \rangle}{\epsilon\epsilon_0 A} \quad (8)$$

where $\vec{\mu}$ is the intrinsic dipole moment of the molecule, μ_{\perp} is its vertical component and ϑ is the angle between the dipole moment vector and the normal to the interface; A is the molecular area, n is the number of surface dipoles.

The dipole moment, μ , of a molecule can be calculated with respect to the centre of mass of the molecule using the following equation:

$$\mu = - \sum_{i=1}^{\text{electrons}} r_i + \sum_{A=1}^{\text{nuclei}} Z_A \cdot R_A \quad (9)$$

where Z_A is the charge of the nuclear core, R_A is the distance between the origin and nucleus A and r_i is the distance between the origin and electron i .

Semi-empirical computations for DPPC polar group provided a value of $|\vec{\mu}^{\text{DPPC}}| = 16.6$ D with AM1 parameterization and $|\vec{\mu}^{\text{DPPC}}| = 14.0$ D with PM3 considering the dipole moment directed along the $^-\text{P}-\text{N}^+$ bond; these values are in good agreement with $|\vec{\mu}^{\text{DPPC}}| = 19$ D found in the literature [38]. Application of Eq. (8) to DPPC monolayers on water subphase in the condensed phase provided an angle $\vartheta=88^\circ$ between $\vec{\mu}^{\text{DPPC}}$ and the normal to the interface, which indicates that the choline polar group lies almost parallel to the surface. The same conclusions were reached by other authors [34,39] that considered separately the contribution of terminal $-\text{CH}_3$, of the carboxylic group, CO, and of the choline moiety. Similar deductions can be made for DPPE, in this case, we computed a dipole moment of $|\vec{\mu}^{\text{DPPE}}| = 9.0$ D and $|\vec{\mu}^{\text{DPPE}}| = 12.9$ D with AM1 and PM3 semi-empirical calculations, respectively. We determined an average angle of 87° between the intrinsic dipole moment of the polar group of DPPE, which is directed along the $^-\text{P}-\text{N}^+$, and the normal to the interface. The choline and the ethanolamine groups are oriented similarly at the interface, the main difference being their steric hindrance: the positive bulky choline group lies deeper in the aqueous phase than the positive diethylammonium of DPPE relative to their

Table 4

Tetracycline surface densities (n_{TC}) and volume/surface partition constants (k_{rip}) as a function of tetracycline concentration in the subphase

[TC], M	$\pi=5 \text{ mN m}^{-1}$						$\pi=35 \text{ mN m}^{-1}$					
	Ψ_0 , mV	ΔV_{TC} , mV	n_{TC} , molec. \AA^{-2}	$n_{\text{DPPA}}/n_{\text{TC}}$	k_{rip} , cm^{-1}	θ°	Ψ_0 , mV	ΔV_{TC} , mV	n_{TC} , molec. \AA^{-2}	$n_{\text{DPPA}}/n_{\text{TC}}$	k_{rip} , cm^{-1}	θ°
1×10^{-6}	−391	4	8.2×10^{-5}	>100	7.3×10^2	84	−396	−2	4.1×10^{-5}	>100	1.5×10^3	92
5×10^{-6}	−378	−5	1.0×10^{-4}	>100	3.0×10^3	91	−384	−7	1.4×10^{-4}	>100	2.2×10^3	94
5×10^{-5}	−336	−73	1.5×10^{-3}	14	2.0×10^3	98	−346	−53	1.1×10^{-3}	23	2.7×10^3	120
1×10^{-4}	−312	−177	3.6×10^{-3}	5	1.7×10^3	98	−328	−154	3.1×10^{-3}	8	1.9×10^3	124
5×10^{-4}	−245	−222	4.5×10^{-3}	3	6.7×10^3	95	−283	−147	3.0×10^{-3}	8	1.0×10^4	112
2×10^{-3}	−209	−251	5.1×10^{-3}	2	2.4×10^4	95	−242	−193	3.9×10^{-3}	6	3.1×10^4	102
5×10^{-3}	−171	−309	6.3×10^{-3}	1.5	4.8×10^4	95	−204	−273	5.6×10^{-3}	3	5.4×10^4	98

phosphate group in agreement with previous reports [39].

ΔV isotherms for DPPA on water change significantly with pH only below pH=3 [37,40,41], even if the term $\Delta V_{\text{dip}}^{\text{Lipid}}$ for DPPA cannot be considered strictly constant throughout all the pH range investigated (2.8–5.7); we assumed that such change should be small.

The dipole moment of the predominant HDPPA[−] species obtained from semi-empirical calculations provided an average value of $\vartheta=85^\circ$ with μ^{HDPPA} directed along the PC bond.

The phosphate group of DPPA is oriented parallel to the interface analogously with what previously discussed for DPPC and DPPE: the polar groups of all three phospholipids almost lie on the plane of the interface with a steric hindrance increasing in the order DPPA<DPPE<DPPC.

3.3.2. Tetracycline-induced surface potential changes for phospholipid monolayers

In Figs. 4–6, the behavior of surface potential ΔV as a function of the phospholipid molecular area is described for some typical tetracycline concentrations.

For DPPC expanded phases, the increase of antibiotic concentration in the subphase promotes a shift of the ΔV isotherms towards higher surface potential values. In the gaseous phase, we observe a poorly reproducible behavior of ΔV – A curves which is probably due to the heterogeneity of the monolayer; interestingly such heterogeneity vanishes with increasing the TC content. On the contrary, in the condensed phases, ΔV is almost unaffected by the presence of TC in the subphase. In fact, ΔV is almost invariant with respect to the TC concentration above $\pi=50 \text{ mN m}^{-1}$. Analysis of π – A isotherms already suggested that above this pressure TC could be pushed down deeper in the diffuse double layer explaining ΔV behavior.

The general features of ΔV – A curves for DPPE are similar to the ones described for DPPC. Major effects are observed for DPPA monolayers: the ΔV curves reported in Fig. 6 show a variation of surface potential both in the expanded and in the condensed phases as compared to pure water subphase, even if the effect is more evident in the expanded phase of DPPA monolayers.

In order to gain a deeper knowledge of the parameters ruling the interaction mechanism, we analyzed the results obtained from ΔV measurements. The three-layer-capacitor model [34,42] subdivides the term $\frac{\mu_{\perp}}{\varepsilon}$ in Eq. (8) into three contributions:

$$\frac{\mu_{\perp}^{\text{TOT}}}{\varepsilon} = \frac{\mu_{\perp}^{\text{H}}}{\varepsilon_{\text{H}}} + \frac{\mu_{\perp}^{\text{W}}}{\varepsilon_{\text{W}}} + \frac{\mu_{\perp}^{\text{T}}}{\varepsilon_{\text{T}}} \quad (10)$$

where μ_{\perp}^{H} is the dipole moment of the polar head group region, μ_{\perp}^{W} is the contribution of oriented water molecules which constitute the hydration shell of lipid head groups at the water/air interface and μ_{\perp}^{T} is the dipole moment of the hydrophobic part; ε_{H} , ε_{T} , ε_{W} , are the local dielectric constant for the head group, tails and interfacial water region, respectively.

According to this model, any variation in ΔV_{dip} can be related either to a change in the orientation of the polar groups, to the water penetration and/or reorganization at the interface or, in our specific case, to the effective interfacial contribution of molecules, i.e. tetracycline, adsorbed or penetrated from the subphase, that is to say:

$$\Delta V = \Delta V_{\text{dip}} + \Psi_0 = \Delta V_{\text{dip}}^{\text{Lipid}} + \Delta V_{\text{dip}}^{\text{TC}} + \Psi_0 \quad (11)$$

$\Delta V_{\text{dip}}^{\text{TC}}$ can be estimated for this equation provided $\Delta V_{\text{dip}}^{\text{Lipid}}$ and Ψ_0 are known.

For DPPC and DPPE $\Psi_0=0$ in Eq. (11) and $\Delta V_{\text{dip}}^{\text{TC}} = \Delta V - \Delta V_{\text{dip}}^{\text{Lipid}} - \Psi_0^{\text{TC}}$; in the case of DPPA rearrangements of Eq. (11) yields:

$$\begin{aligned} \Delta V_{\text{dip}}^{\text{TC}} &= \Delta V - \left(\Delta V_{\text{dip}}^{\text{Lipid}} + \Psi_0^{\text{Lipid}} \right) - \Psi_0^{\text{TC}} \\ &= \Delta(\Delta V) - \Delta\Psi_0 \end{aligned} \quad (12)$$

We considered the term $\Delta V_{\text{dip}}^{\text{Lipid}}$ not affected by the presence of tetracycline at the interface for the three phospholipids. First of all, π and γ measurements showed that the amount of TC in the monolayer is expected to be small; therefore we considered negligible the term Ψ_0^{TC} for all the examined systems. This assumption is further justified considering the single terms of Eq. (10): although the term $\mu_{\perp}^{\text{W}}/\varepsilon_{\text{W}}$ might change as a function of TC content, it is known from previous work that this contribution is negligible with respect to the other ones [39]. Secondly, penetration of TC in the compact hydrophobic layer is unlikely to

occur, as shown in Section 3.2) from area requirements considerations, and the term $\frac{\mu_{\perp}}{\varepsilon_{\text{T}}}$ in Eq. (10) can be considered constant.

The head group contribution, $\mu_{\perp}^{\text{H}}/\varepsilon_{\text{H}}$, might vary due to changes either in the carboxylic and phosphatidic regions; since penetration of tetracycline in the monolayer was excluded we considered negligible any effect on the CO group. Besides, the phosphatidic group contribution can be considered constant below 2×10^{-3} M; below this concentration the neutral DPPA species contribution is lower than 4%, and basically only HDPPA[−] is present.

Ψ_0 values obtained from Eq. (12) together with the corresponding ΔV at maximum packing are reported in Table 4 for each tetracycline concentration.

We attempted to isolate the contribution of tetracycline to ΔV in three different regions of the isotherms: gaseous phases ($\pi \approx 0$), liquid-expanded phases ($\pi = 5 \text{ mN m}^{-1}$) and condensed phases ($\pi = 35 \text{ mN m}^{-1}$).

3.3.3. Gaseous phases

Interestingly, we found a prompt increase in surface potential (250 mV) also at very low phospholipid surface density in the case of high tetracycline content, i.e. high H₄TC⁺ concentration, whereas for extremely expanded phospholipid monolayers on water the surface potential is basically zero. This enhancement of ΔV can be ascribed either to a perturbation of the network of water molecules at the interface and/or to the double layer term, Ψ_0 , or to the presence of TC at the interface. In particular many authors [43,44] ascribe the onset of the surface potential to the formation of a hydrogen-bond network. Indeed, the increase of the onset area with increasing tetracycline may indicate that the antibiotic is participating in the network between the phospholipid head groups adsorbing at the interface. Under the crude assumption that the major effect is due solely to the presence of tetracycline dipoles, we attempted to evaluate the contribution of tetracycline to the surface potential in the expanded region of ΔV – A isotherms for the highest TC concentration where only the charged H₄TC⁺ species is present.

We used ΔV values of 200 mV for DPPC, 250 mV for DPPE and 200 mV for DPPA corresponding to molecular area values of $220 \text{ \AA}^2 \text{ molecule}^{-1}$, $105 \text{ \AA}^2 \text{ molecule}^{-1}$ and $150 \text{ \AA}^2 \text{ molecule}^{-1}$ for DPPC, DPPE

and DPPA, respectively. Considering that in the adsorption film (see Section 3.1) tetracycline occupies an area of 100 – 158 \AA^2 at most one tetracycline molecule per phospholipid molecule is present at the molecular areas listed above. Application of Eq. (8) with $n=1$, provided values $\mu_{\perp}^{\text{TC}} = 1167 \text{ mD}$ for DPPC, $\mu_{\perp}^{\text{TC}} = 696 \text{ mD}$ for DPPE and $\mu_{\perp}^{\text{TC}} = 1409 \text{ mD}$ for DPPA.

The orientation of the TC molecule with respect to the interface may be evaluated, provided μ is known. The dipole moment of tetracycline was computed for both the H₃TC and the H₄TC⁺ forms, we obtained similar values of 14.8 D but different spatial orientation, the μ^{TC} vectors for H₄TC⁺ and H₃TC are depicted in Fig. 3. A positive ΔV contribution implies that the TC amino group (see Fig. 3) points towards the air region. Substitution of μ^{TC} value in Eq. (8) allowed to determine ϑ , the angle between the normal to the interface and the molecular dipole moment. ϑ falls in the range 85 – 89° to indicate that the plane of the BCD rings is almost parallel to the interface plane in agreement with surface tension results.

3.3.4. Liquid expanded and highly condensed phases

Variations of the surface potential of DPPC and DPPE as function of TC content in the subphase, at $\pi = 5 \text{ mN m}^{-1}$ and $\pi = 35 \text{ mN m}^{-1}$, are reported in Fig. 8. We distinctly identify a discontinuity in ΔV behavior at a threshold concentration $[\text{TC}]^* \approx 5 \times 10^{-4} \text{ M}$ as in the case of ΔA data. ΔV increases sharply at low TC concentration and reaches a constant value at $[\text{TC}]^*$, then surface potential decreases slowly for DPPE and more significantly for DPPC. We recall that H₃TC is in excess below $[\text{TC}]^*$, whereas above $[\text{TC}]^*$ the charged species, H₄TC⁺, becomes dominant. The contribution of H₃TC (and H₄TC⁺) to the surface potential can be estimated from Eq. (11), similar models were used also by other author for cationic drugs [45].

For DPPC and DPPE $\Psi_0=0$ in Eq. (11) and the increase in ΔV below $[\text{TC}]^*$ can be ascribed to the migration of H₃TC, the predominant species in solution, towards the interface. At any rate, this term $\Delta V_{\text{dip}}^{\text{TC}} = \Delta V - \Delta V_{\text{dip}}^{\text{Lipid}}$ is very small and comparable to the experimental error in ΔV measurements suggesting that tetracycline contribution at the interface is negligible; these findings are in agreement with the results of the analysis of ΔA values.

At concentrations higher than $[TC]^*$, H_4TC^+ predominates, and presumably its interactions with the negative charge localized on the readily accessible P^- atom of the polar groups become more important, this effect is clearly reflected in the increase in ΔA (Fig. 7). Surprisingly, the effect of a further increase in H_4TC^+ concentration at the interface induces a reduction of ΔV values (Fig. 8). The data of Section 3.2 indicate that such reduction cannot be interpreted in terms of depletion of TC from the interface, moreover the calculated modulus for H_4TC^+ dipole moment and its orientation at the interface would result in a vertical component of the dipole moment comparable to the one observed for the zwitterionic H_3TC (see Fig. 3). In order to explain the reduction of ΔV , we should take into consideration, besides the negligible Ψ_0 contribution due to TC at the interface and a small contribution to the term μ_{\perp}^W/ϵ_W , other terms such as the reorientation of the polar groups, which is associated to a decrease of the term μ_{\perp}^H/ϵ_H . In fact, reorientation of the choline group with the $N(CH_3)_3^+$ deeper in the water phase would induce a decrease of the vertical component of the dipole moment of DPPC and, at the same time, it would provide more space to allow H_4TC^+ to interact with the negative phosphorus region of the monolayer. Similar results were also obtained from NMR and IR spectroscopy for the interaction of phloretin molecule with DPPC monolayer [5,46]. The role of the reorientation of the polar group is supported also by the results obtained for DPPE monolayers for concentrations higher than $[TC]^*$. In this case, the decrease of ΔV is much lower and it correlates to the fact that H_4TC^+ can insert more easily at the interface without inducing major changes in the orientation of the small phosphatidylethanolamine group.

The effect of the increase of H_4TC^+ species at the air–water interface on monolayer features is strongly enhanced in the case of DPPA, whose protonation equilibria changes with the pH of the subphase. The behavior of ΔV as a function of TC content in the subphase is reported in Fig. 9. ΔV increases to reach a plateau (350–370 mV) value at $[TC]=1 \times 10^{-4}$ M, after this concentration the surface potential drastically decreases to 240 mV. This concentration value marks a discontinuity in ΔV behavior and corresponds to the threshold value previously discussed. It is interesting

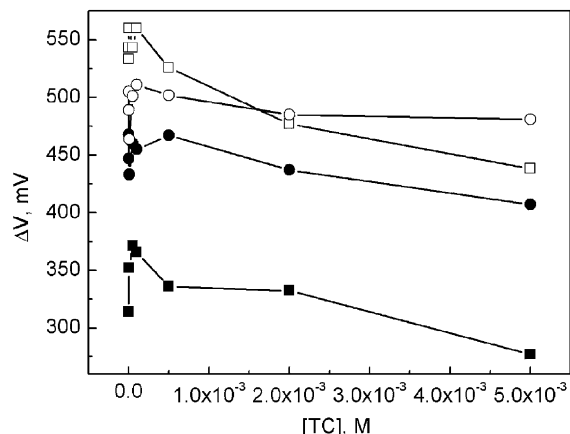


Fig. 8. Surface potentials at constant π of DPPC and DPPE monolayers vs. tetracycline concentration: DPPC (squares) and DPPE (circles) at $\pi=5$ mN m⁻¹ (filled symbols) and at $\pi=35$ mN m⁻¹ (open symbols).

to note that, differently from DPPC and DPPE, $[TC]^*$ shifts to lower values, that is 1×10^{-4} M, this feature suggests that, besides the H_3TC – H_4TC^+ transition, protonation equilibria of DPPA are involved. In fact pH=4, that is to say $[TC]=[TC]^*$, corresponds to a maximum for the fraction of $HDPPA^-$, at the same time the $DPPA^{2-}$ form is replaced with the neutral form. After the threshold concentration, ΔV increases again indicating that interactions between the couple $H_4TC^+/DPPA$ are enhanced compared to $H_3TC/DPPA$, the minimum of ΔV is observed for the highest concentration of $HDPPA^-$ coupled with a large concentration of neutral H_3TC .

The values of ΔV_{dip}^{TC} from Eq. (11) in closely packed phases are reported in Table 4. In order to estimate tetracycline concentration at the interface, we correlated the surface potential to the dipole surface density using two different procedures. In the first one, we assumed that tetracycline adopts a flat-like orientation at the interface, similar to what reported above for $\pi=0$, also in the condensed phase, we utilized $|\vec{\mu}| = 14.8$ D from HyperChem calculations considering ϑ values in the range 85–88°. We obtained n_{TC} values reported in Table 4 together with the molar ratio between DPPA and tetracycline, a reasonably good agreement is found with the values obtained from the behavior of ΔA (see Table 3). From n_{TC} values it is possible to evaluate a volume/surface

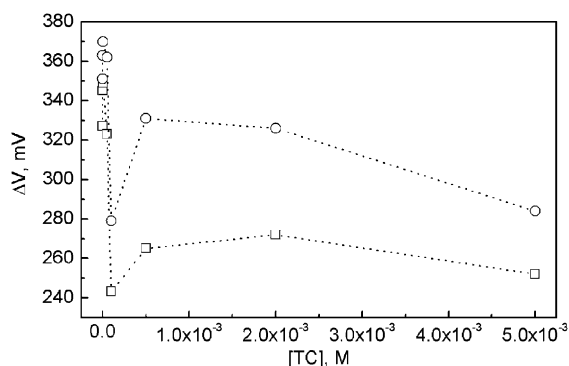


Fig. 9. Surface potentials at constant π of DPPA monolayers vs. tetracycline concentration: $\pi=5 \text{ mN m}^{-1}$ (squares), $\pi=35 \text{ mN m}^{-1}$ (circles).

partition constant, k_{rip} defined as the ratio between surface concentration and bulk concentration

$$k_{\text{rip}} = \frac{n_{\text{TC}}}{n_{\text{TC}}^{\text{bulk}}} \quad (13)$$

k_{rip} values, reported in Table 4, are of the same order of magnitude of k_{rip} determined for interfacial enzymatic reactions reported in the literature [7]. k_{rip} value increases as a function of TC bulk content to a saturation limit for $[\text{TC}]=1 \times 10^{-4} \text{ M}$, whereas after this concentration we record an almost linear increase of k_{rip} . The partition model does not account for the experimental data above $[\text{TC}]^*$ probably because of simultaneous presence of different TC species. The results suggest that the H_4TC^+ species, the predominant form above $[\text{TC}]^*$, interacts more strongly than H_3TC with HDPPA^- , which in turn remains the prevalent species at the interface over the entire TC concentration range studied.

In the second procedure, we calculated $\mu_{\perp}^{\text{TC}} = \varepsilon \varepsilon_0 \Delta V_{\text{dip}}^{\text{TC}} / n_{\text{TC}}$ employing the surface density of TC computed from the data obtained from the analysis of π - A isotherms reported in Table 3. In this way no assumptions were imposed on the magnitude and direction of tetracycline dipole moment. The angle between tetracycline dipole moment and the normal to the interface was also obtained and the corresponding values are reported in Table 4. We found that although the orientation of tetracycline remains essentially flat, the direction of the dipole reverses, implying that the positive end of the calculated μ^{TC} localized on the

dimethylamino group, is below the water surface. This orientation of tetracycline would allow strong interactions to be established with the negatively charged phosphate group of DPPA.

The previous results converge in identifying electrostatic interactions between the two species of tetracycline and the phospholipid as the driving force for tetracycline association at the interface. We therefore suggest that tetracycline may be either adsorbed underneath the polar head group region, or partly integrated among the polar groups excluding penetration. Similarly, previous works [47] demonstrated that the poorly hydrophobic antibiotics are unable to cross the lipid region and remain adsorbed to the polar head group through electrostatic interactions. In the present work, we have confined our approach to a semi-qualitative description of the process, a more detailed study is still in progress where the individual contribution of the different TC species are isolated and quantified.

4. Conclusions

The results reported and discussed above allow to draw some general conclusions on the mechanism of interaction of tetracycline with phospholipid monolayers at water–air interface.

Tetracycline was found to have a very small tendency to accumulate at the interface in the absence of any amphiphilic monolayer. Migration towards the interface is promoted in the presence of the phospholipids and it is basically due to electrostatic reasons. In fact we observed higher interactions in the series $\text{DPPE} < \text{DPPC} < \text{DPPA}$. This effect is particularly important in the expanded phase and for tetracycline concentrations higher than a critical threshold value. Such threshold value coincides for DPPC and DPPE and it corresponds to the pH at which the charged species H_4TC^+ becomes predominant. For DPPA, the threshold value is lower ($[\text{TC}]=1 \times 10^{-4} \text{ M}$), because in this case the change in pH due to the increase of TC in the subphase promotes also a shift towards the negatively charged form of DPPA. Large interactions between HDPPA^- and H_4TC^+ are established as shown by the increase in surface areas per DPPA molecule and surface potential behavior.

This work is an example of how adsorbable substances can be organized at water–air interface by the interplay of electrostatic interactions. Such interactions, although strong enough to persist also in the condensed phase, do not seem sufficient to promote penetration of TC through the polar groups up hydrophobic layer. For this reason, crossing of the tetracycline through the cellular membrane appear unreasonable in the absence of suitable carrier or protonic units. This is in agreement with previous studies that reported that the most abundant resistance mechanism against tetracyclines in gram-negative bacteria is based on the active export of TC out of the cytoplasm by the intrinsic membrane protein TetA [48,49].

Our data suggest that tetracycline migrates at the interface and is adsorbed underneath, or partly associated with, the polar head groups of the phospholipids. From the comparison of experimental data with semi-empirical calculation we could sketch a distribution of tetracycline below the polar head group of DPPA in a flat-like orientation, maximum incorporation is reached in the condensed phase where a molar ratio 2:1 between the phospholipid and the charged species of tetracycline is found.

The quantitative interpretation of the results of the present work is hindered by the change in the distribution of the different protonated species with increasing tetracycline concentration. Further insight on the details of this mechanism will be presented in a separate work where pH, and thus protonation of DPPA, will be kept constant.

Nevertheless, the present study provides an important piece of information on tetracycline interactions with natural membranes since during extracellular trafficking the antibiotic is likely to encounter milieu in which pH might vary modulating the interactions with membrane phospholipids. Moreover, these first results appear promising in the selection of a candidate monolayer for biomimetic sensor for tetracycline.

Acknowledgements

The work was supported by the Italian Ministry of Health, by MIUR (Ministero dell' Istruzione, dell' Università e della Ricerca). Thanks are due to Dr Silvia Bini for her help in the study of bulk equilibria of tetracycline.

References

- [1] C. Krafft, W. Hinrichs, P. Orth, W. Saenger, H. Welfle, Interaction of Tet repressor with operator DNA and with tetracycline studied by infrared and Raman spectroscopy, *Biophys. J.* 74 (1998) 63–71.
- [2] T.H. Ha, C.H. Kim, J.S. Park, K. Kim, Interaction of indolicidin with model lipid bilayer: quartz crystal microbalance and atomic force microscopy study, *Langmuir* 16 (2000) 871–875.
- [3] C. Mestres, M.A. Alsina, M.A. Busquets, I. Murányi, F. Reig, Interaction of colistin with lipids in liposomes and monolayers, *Int. J. Pharm.* 160 (1998) 99–107.
- [4] T. Guilmin, E. Goormaghtigh, R. Brasseur, J. Casper, J.M. Ruyschaert, Evaluation of the anesthetic-lipid association constant. A monolayer approach, *Biochim. Biophys. Acta* 685 (1982) 169–176.
- [5] T. Yoshida, Y. Koga, H. Minowa, H. Kamaya, I. Ueda, Interfacial lateral electrical conductance on lipid monolayer: dose-dependent converse effect of alcohols, *J. Phys. Chem. B* 104 (2000) 1249–1252.
- [6] S. Lieberman, V.V.K. Prasad, L. Ponticorvo, Lipophilic complexes of pharmacologically active inorganic mineral acid esters of organic compounds, PA 5002936, 1991.
- [7] A. Baszkin, W. Norde, *Physical Chemistry of Biological Interfaces*, Plenum press, New York, 2000.
- [8] T. Söderlund, J.Y.A. Lehtonen, P.K.J. Kinnunen, Interactions of cyclosporin A with phospholipid membranes: effect of cholesterol, *Mol. Pharmacol.* 55 (1999) 32–38.
- [9] G.L. Gaines Jr, *Insoluble Monolayers at Liquid–Gas Interfaces*, John Wiley and Sons, New York, 1966.
- [10] G. Gabrielli, G. Caminati, M. Puggelli, Interactions and reactions of monolayers and Langmuir–Blodgett multilayers with compounds in the bulk phase, *Adv. Colloid Interface Sci.* 87 (2000) 75–111.
- [11] M.J.S. Dewar, C.H. Reynolds, An improved set of MNDO parameters for sulfur, *J. Comp. Chem.* 7 (1986) 140–147.
- [12] J.J.P. Stewart, Optimization of parameters for semiempirical methods. I. Method, *J. Comp. Chem.* 10 (1989) 209–220.
- [13] J.M. Wessels, W.E. Ford, W. Szymczak, S. Scheneider, The complexation of tetracycline and anhydrotetracycline with Mg^{2+} and Ca^{2+} : a spectroscopic study, *J. Phys. Chem. B* 102 (1998) 9323–9331.
- [14] J.R.D. McCormick, S.M. Fox, L.L. Smith, B.A. Bitler, J. Reichenthal, V.E. Origoni, et al., The reversible epimerization occurring in the tetracycline family. The preparation, properties and proof of structure of some 4-epitetracyclines, *J. Am. Chem. Soc.* 79 (1957) 2849–2858.
- [15] L.J. Leeson, J.E. Krueger, R.A. Nash, Structural assignment of the second and third acidity constants of tetracycline antibiotics, *Tetrahedron Lett.* 18 (1963) 1155–1160.
- [16] W.A. Baker Jr, P.M. Brown, Metal binding in tetracyclines. Cobalt(II) and nickel(II) complexes, *J. Am. Chem. Soc.* 88 (1966) 1314–1317.
- [17] J. Gulbis, G.W. Everett Jr, Metal binding characteristics of tetracycline derivatives in DMSO solution, *Tetrahedron* 32 (1976) 913–917.
- [18] H.A. Duarte, S. Carvalho, E.B. Paniago, A.M. Simas, Impor-

- tance of tautomers in the chemical behavior of tetracyclines, *J. Pharm. Sci.* 88 (1999) 111–120.
- [19] L. Lambs, B. Decock-Le Reverend, H. Kozlowski, G. Berthon, Metal ion-tetracycline interactions in biological fluids. 9. Circular dichroism spectra of calcium and magnesium complexes with tetracycline, oxytetracycline, doxycycline and chlortetracycline and discussion of their binding modes, *Inorg. Chem.* 27 (1988) 3001–3012.
- [20] A. Seelig, Local anaesthetics and pressure: a comparison of dibucaine binding to lipid monolayers and bilayers, *Biochim. Biophys. Acta* 899 (1987) 196–204.
- [21] C. Gumila, G. Miquel, P. Seta, M.-L. Ancelin, A.-M. Delort, G. Jeminet, et al., Ionophore–phospholipid interactions in Langmuir films in relation to ionophore selectivity toward plasmodium-infected erythrocytes, *J. Colloid Interface Sci.* 218 (1999) 377–387.
- [22] R. Aveyard, D.A. Haydon, *An Introduction to the Principles of Surface Chemistry*, Cambridge University Press, 1973.
- [23] P.J. Lukes, M.C. Petty, J. Yarwood, An infrared study of the incorporation of ion channel forming peptides into Langmuir–Blodgett films of phosphatidic acid, *Langmuir* 8 (1992) 3043–3050.
- [24] H. Nakahara, K. Fukuda, H. Akutsu, Y. Kyogoku, Monolayers and multilayers of phosphatidylethanolamine: effects of spreading solvent, monovalent cations and substrate pH, *J. Colloid Interface Sci.* 65 (1978) 517–526.
- [25] J.M. Solletti, M. Botreau, F. Sommer, W.L. Brunat, S. Kasas, T.M. Duc, et al., Elaboration and characterization of phospholipid Langmuir–Blodgett films, *Langmuir* 12 (1996) 5379–5386.
- [26] J.T. Davies, E.K. Rideal, *Interfacial Phenomena*, Academic Press, New York, 1963.
- [27] B. Wetzter, A. Pfandler, E. Györvary, D. Pum, M. Lösche, U.B. Sleytr, S-layer reconstitution at phospholipid monolayers, *Langmuir* 14 (1998) 6899–6906.
- [28] M.L.F. Ruano, K. Nag, C. Casals, J. Perez-Gil, K.M.W. Keough, Interactions of pulmonary surfactant protein A with phospholipid monolayers change with pH, *Biophys. J.* 77 (1999) 1469–1476.
- [29] F. Wang, S.F. Sui, Phase separation of phospholipid monolayers induced by membrane penetration of human apolipoprotein H, *Colloid Surf. A* 98–200 (2002) 281–286.
- [30] S. Brancato, A. Serfis, Incorporation of blood-clotting proteins into phospholipid Langmuir monolayers: a fluorescence microscopy study, *J. Colloid Interface Sci.* 239 (2001) 139–144.
- [31] S. Sivakesava, J. Irudayaraj, Rapid determination of tetracycline in milk by FT-MIR and FT-NIR spectroscopy, *J. Dairy Sci.* 85 (2002) 487–493.
- [32] S. Banerjee, M. Bennouna, J. Ferreira-Marques, J.M. Ruyschaert, J. Caspers, Lipid–drug interaction and colligative properties in phospholipid vesicles, *J. Colloid Interface Sci.* 219 (1999) 168–177.
- [33] M. Bennouna, J. Ferreira-Marques, S. Banerjee, J. Caspers, J.M. Ruyschaert, Interaction of chlorpromazine with phospholipid membranes: a monolayer and a microelectrophoresis approach, *Langmuir* 13 (1997) 6533–6539.
- [34] D.M. Taylor, O. Novais De Oliveira Jr, H. Morgan, Models for interpreting surface potential measurements and their application to phospholipid monolayers, *J. Colloid Interface Sci.* 139 (1990) 508–518.
- [35] D. Ducharme, J.-J. Max, C. Salesse, R.M. Leblanc, Ellipsometric study of the physical states of phosphatidylcholines at the air–water interface, *J. Phys. Chem.* 94 (1990) 1925–1932.
- [36] E.D. Goddard, Ionizing monolayers and pH effects, *Adv. Colloid Interface Sci.* 4 (1974) 45–78.
- [37] R.C. Ahuja, P.L. Caruso, D. Möbius, G. Wildburg, H. Ringsdorf, D. Philp, et al., Molecular organization via ionic interactions at interfaces. 1. Monolayers and LB films of cyclic bisbipyridinium tetracations and dimyristoylphosphatidic acid, *Langmuir* 9 (1993) 1534–1544.
- [38] J.F. Tocanne, J. Teissie, Ionization of phospholipids and phospholipid-supported interfacial lateral diffusion of protons in membrane model systems, *Biochim. Biophys. Acta* 1031 (1990) 111–142.
- [39] J.G. Petrov, E.E. Polymeropoulos, H. Möhwald, On the tri-capacitor model for surface potential of insoluble monolayers, *J. Phys. Chem.* 100 (1996) 9860–9869.
- [40] H. Abriouel, J. Sánchez-González, M. Maqueda, A. Gálvez, E. Valdivia, M.J. Gálvez-Ruiz, Monolayer characteristics of bacteriocin AS-48, pH effect and interactions with dipalmitoyl phosphatidic acid at the air–water interface, *J. Colloid Interface Sci.* 233 (2001) 306–312.
- [41] D. Papahadjopoulos, Surface properties of acidic phospholipids: interaction of monolayers and hydrated liquid crystals with uni- and bi-valent metal ions, *Biochim. Biophys. Acta* 163 (1968) 240–254.
- [42] R.J. Demchak, T. Fort Jr., Surface dipole moments of close-packed non-ionized monolayers at the air–water interface, *J. Colloid Interface Sci.* 46 (1974) 191–202.
- [43] V.B.P. Leite, A. Cavalli, O.N. Oliveira Jr., Hydrogen-bond control of structure and conductivity of Langmuir films, *Phys. Rev. E* 57 (1998) 6835–6839.
- [44] C. Lambruschini, A. Relini, A. Ridi, L. Cordone, A. Gliozzi, Trehalose interacts with phospholipid polar heads in langmuir monolayers, *Langmuir* 16 (2000) 5467–5470.
- [45] S. Banerjee, J. Caspers, M. Benneouna, A.M. Sauterau, J.F. Tocanne, J.M. Ruyschaert, Evaluation of drug–lipid association constants from microelectrophoretic mobility measurements, *Langmuir* 11 (1995) 1134–1137.
- [46] S. Diaz, F. Lairion, J. Arroyo, A.C. Biondi De Lopez, E.A. Disalvo, Contribution of phosphate groups to the dipole potential of dimyristoylphosphatidylcholine membranes, *Langmuir* 17 (2001) 852–855.
- [47] C. Heywang, M. Saint-Pierre Chazalet, M. Masson, J. Bolard, SERR study of the interaction of anthracyclines with mono- and bilayers of charged phospholipids, *Langmuir* 13 (1997) 5634–5643.
- [48] M. Kaneko, A. Yamaguchi, T. Sawai, Energetics of tetracycline efflux system encoded by Tn10 in *Escherichia coli*, *FEBS Lett.* 193 (1985) 194–198.
- [49] A. Yamaguchi, T. Udagawa, T. Sawai, Transport of divalent cations with tetracycline as mediated by the transposon Tn10-encoded tetracycline resistance protein, *J. Biol. Chem.* 265 (1990) 4809–4813.